C- and O-Bonded Carbon Monoxide on Surfaces: Interactions of $[CpW(CO)_3]^-$ with Cations on Magnesia, Alumina, and Potassium-Modified Alumina

Mark M. Otten and H. Henry Lamb*

Contribution from the Department of Chemical Engineering, North Carolina State University, Raleigh, North Carolina 27695-7905

Received August 26, 1993®

Abstract: Surface-bound $[CpW(CO)_3]^-$ complexes were prepared by deprotonation of $[HCpW(CO)_3]$ on MgO, γ-Al_2O_3, and K/Al_2O_3 and characterized by infrared and extended X-ray absorption fine structure (EXAFS) spectroscopies. On the metal oxide surfaces, $[CpW(CO)_3]^-$ interacts with coordinatively unsaturated cations via C- and O-bonded carbonyl ligands. A carbonyl O atom can be envisaged as completing the coordination sphere of a $\{M^{n+}\}$ ion terminating the bulk metal oxide. Ion adducts containing one Σ–CO– ligand per complex are formed on each metal oxide; this parallels the solution ion-pair chemistry of $[CpW(CO)_3]^-$ with K^+, Mg^{2+}, and Al^{3+}. On highly dehydroxylated MgO and γ-Al_2O_3, novel bis(isocarbonyl) adducts are formed in which the $[CpW(CO)_3]$ moiety is inferred to bridge $\{M^{n+}\}$ ions via Σ–CO– ligands. The crystallographically characterized compound $[(AlMe_2)CpW(CO)_3]_2$ is cited as precedent for this bonding geometry in solution organometallic chemistry.

Introduction

Fundamental investigations of organometallic chemistry on metal oxide surfaces are providing basic data for the design of supported "molecular" catalysts and are leading to better understanding of surface structures and intermediates in supported metal catalysis.[1-4] The surface organometallic chemistry of metal clusters and mononuclear metal complexes on typical catalyst supports often is determined by the acid–base properties of the metal oxide.[4] On basic metal oxide surfaces, chemisorption of binary and hydrido carbonyls generally results in the formation of metal carbonyl anions.[5-7] Typically, the ν_{CO} infrared spectra of surface-bound metal carbonylates do not agree closely with those of the free anionic complexes in solution. On the basis of the resemblance of the spectra to those of contact ion pairs in nonpolar solvents, a secondary acid–base interaction involving basic carbonyl O atoms and coordinatively unsaturated cations $\{M^{n+}\}$[8] (Lewis acid centers) has been proposed.[5,7] As ion-pairing effects on reactivity are well established in solution organometallic chemistry,[9] this type of interaction is expected to influence the reactivity of the surface-bound metal carbonylates. Moreover, the surface-bound anions might be used to probe Lewis acid centers on surfaces, and the surface structures might serve as models for C- and O-bonded intermediates in CO hydrogenation catalysis.

Detailed analyses of the ν_{CO} infrared spectra of alkali metal, Mg, and Al salts of metal carbonyl anions (e.g., $[Co(CO)_4]^-$ and $[CpM'(CO)_3]^-$ (M' = Cr, Mo, W)) in ethereal solutions have demonstrated that the ion pairs are linked by $M'CO\cdots M^{n+}$ carbonyl bridges.[9] End-on C- and O-bonded carbonyl ligands (designated Σ–CO–) resulting from interaction of a metal cation or a molecular Lewis acid with a carbonyl O atom are well-known in solution organometallic chemistry, and crystal structures have been reported for a number of isocarbonyl compounds.[10] Edgell and co-workers have used ion-pairing effects on the ν_{CO} infrared spectra of mononuclear carbonyl anions to probe the coordination environments of metal counter cations in solution,[11] and in prospect, metal carbonyl anions can be valuable probes of cation environments on metal oxide surfaces.

C- and O-bonded carbon monoxide species are thought to be important intermediates in homogeneous[12] and heterogeneous[13-16] CO reduction catalysis, particularly in the synthesis of oxygen-containing organic compounds. Vibrational spectroscopy has been most useful in identifying these species in solution and on surfaces, owing to their unusually low CO stretching frequencies. For the soluble organometallics, X-ray crystallography and NMR spectroscopy have been used to further elucidate the structures. C- and O-bonded carbonyl species on metal single crystals,[17-19] heterometal-decorated single crystals,[20] and supported metal catalysts[13-15,21] have been detected by vibrational spectroscopy, but in comparison to their molecular organometallic analogues, bonding in these surface species is not well understood. The surface species may be Σ–CO– bonded or "tilt-adsorbed" (π–CO bonded) at surface steps or at heterobimetallic sites.

Herein, we describe the synthesis and characterization of supported organotungsten complexes that are linked to metal

* To whom correspondence should be addressed.

® Abstract published in *Advance ACS Abstracts*, February 1, 1994.

(1) Basset, J. M.; Candy, J. P.; Choplin, A.; Didillon, B.; Quignard, F.; Theolier, A. In *Perspectives in Catalysis*, Thomas, J. M., Zamaraev, K. I., Eds.; Blackwell Scientific Publications: Oxford, 1992.
(2) Psaro, R.; Ugo, R. In *Metal Clusters in Catalysis*; Gates, B. C., Guczi, L., Knözinger, H., Eds.; Elsevier: New York, 1986.
(3) *Tailored Metal Catalysts*; Iwasawa, Y., Ed.; D. Reidel: Boston, 1986.
(4) (a) Lamb, H. H.; Gates, B. C.; Knözinger, H. *Angew. Chem., Int. Ed. Engl.* **1988**, *27*, 1127. (b) Gates, B. C.; Lamb, H. H. *J. Mol. Catal.* **1989**, *52*, 1.
(5) Hugues, F.; Basset, J. M.; Ben Taarit, Y.; Choplin, A; Primet, M.; Rojas, D.; Smith, A. K. *J. Am. Chem. Soc.* **1982**, *104*, 7020.
(6) Guglielminotti, E.; Zecchina, A. *J. Mol. Catal.* **1984**, *24*, 331.
(7) Lamb, H. H.; Gates, B. C. *J. Am. Chem. Soc.* **1986**, *108*, 81.
(8) Braces are used to designate species terminating the bulk metal oxide.
(9) Darensbourg, M. Y. *Prog. Inorg. Chem.* **1985**, *33*, 221.
(10) Horwitz, C. P.; Shriver, D. F. *Adv. Organomet. Chem.* **1984**, *23*, 219.
(11) Edgell, W. F. In *Infrared and Raman Studies of Ions and Ion Pairs;* Szwarc, M., Ed.; Wiley: New York, 1972; Vol I.
(12) (a) Shriver, D. F. *ACS Symp. Ser.* **1981**, *152*, 1. (b) Richmond, T. G.; Basolo, F.; Shriver, D. F. *Inorg. Chem.* **1982**, *21*, 1272.
(13) (a) Ichikawa, M.; Lang, A. J.; Shriver, D. F.; Sachtler, W. M. H. *J. Am. Chem. Soc.* **1985**, *107*, 7216. (b) Sachtler, W. M. H.; Ichikawa, M. *J. Phys. Chem.* **1986**, *90*, 4752.
(14) Mazzocchia, C.; Gronchi, P.; Tempesti, E.; Guglielminotti, E.; Zanderighi, L. *J. Mol. Catal.* **1990**, *60*, 283.
(15) Xiao, F.-S.; Fukuoka, A.; Ichikawa, M. *J. Catal.* **1992**, *138*, 206.
(16) Haller, G. L.; Resasco, D. E. *Adv. Catal.* **1989**, *36*, 173.
(17) Seip, U.; Tsai, M.-C.; Christmann, K.; Küppers, J.; Ertl, G. *Surf. Sci.* **1984**, *139*, 29.
(18) Shinn, N. D.; Madey, T. E. *J. Chem. Phys.* **1985**, *83*, 5928.
(19) Colaianni, M. L.; Chen, J. G.; Weinberg, W. H.; Yates, J. T., Jr. *J. Am. Chem. Soc.* **1992**, *114*, 3735.
(20) Chen, J. G.; Crowell, J. E.; Ng, L.; Basu, P.; Yates, J. T., Jr. *J. Phys. Chem.* **1988**, *92*, 2574.
(21) Ichikawa, M.; Fukushima, T. *J. Phys. Chem.* **1985**, *89*, 1564.

0002-7863/94/1516-1372$04.50/0

Table 1. Adsorption of $[HCpW(CO)_3]$ on Basic Metal Oxides

metal oxide	pretreatment conditions	surface area (m^2/g)	surface density (complexes/nm^2)
MgO	800 °C, *in vacuo*	39	0.65, 1.3
γ-Al_2O_3	800 °C, *in vacuo*	76	0.65
	400 °C, *in vacuo*	100	0.49
K/Al_2O_3 (1.6 K/nm^2)	800 °C, *in vacuo*	95	0.52
K/Al_2O_3 (7.2 K/nm^2)	800 °C, *in vacuo*	90	0.54

oxide surfaces via Σ–CO– ligands. The surface-bound anions are analogues of contact ion pairs formed by $[CpW(CO)_3]^-$ and K^+, Mg^{2+}, and Al^{3+} ions in nonpolar solvents. We refer to the surface-bound anions as ion adducts to differentiate them from ion pairs and higher order aggregates in solution, where formal charge balance is maintained. On metal oxide surfaces, O coordination of one and two carbonyl ligands of $[CpW(CO)_3]^-$ by $\{M^{n+}\}$ is observed.

Results

Chemisorption of $[HCpW(CO)_3]$ from Solution by Deprotonation. Adsorption of $[HCpW(CO)_3]$ from toluene solution onto MgO, γ-Al_2O_3, and K/Al_2O_3 resulted in chemisorption at the average surface densities given in Table 1. In each case, uptake of the hydride from solution was quantitative; there were no soluble W carbonyl byproducts; and no W carbonyl species were removed by washing with fresh toluene.

Surface deuteroxyl groups $\{OD^-\}$ were produced by adsorption of $[DCpW(CO)_3]$ on MgO, as evidenced by the ν_{OD} spectra of freshly prepared samples. At 0.65 W complexes/nm^2, strong ν_{OD} bands are observed at 2710 and 2615 cm^{-1}. These bands are assigned to isolated and vicinal $\{OD^-\}$, respectively.[22] At a higher coverage (1.3 W complexes/nm^2), a ν_{OD} band at 2590 cm^{-1} is predominant, with strong bands also observed at 2710, 2655, and 2555 cm^{-1}. The predominant band is assigned to $\{Mg^{2+}\}$-coordinated HOD; the other bands are assigned to isolated $\{OD^-\}$, vicinal $\{OD^-\}$, and submonolayer physisorbed HOD, respectively.[22,23] Infrared spectra obtained following adsorption of $[DCpW(CO)_3]$ on highly dehydroxylated γ-Al_2O_3 contained only broad ν_{OD} bands in the 2750–2400-cm^{-1} region, and band assignments were not attempted.

Surface-bound anions were solubilized by cation metathesis with [PPN][Cl] in dichloromethane to yield solutions of $[PPN][CpW(CO)_3]$ (ν_{CO} = 1890 s, 1770 vs cm^{-1}). Infrared spectra of the solids after treatment and rinsing with fresh dichloromethane indicated that all metal carbonyl species had been removed. Control experiments established that W carbonyl species were not removed from MgO and K/Al_2O_3 samples by washing with dichloromethane, but small amounts of $[HCpW(CO)_3]$ were isolated from γ-Al_2O_3 samples by this procedure.

These results demonstrate that adsorption of $[HCpW(CO)_3]$ from toluene solution occurs via reaction with basic $\{O^{2-}\}$ and $\{OH^-\}$ groups. At low coverages on highly dehydroxylated surfaces, the deprotonation reaction can be written as

$$[HCpW(CO)_3] + \{M^{n+}\}_x\{O^{2-}\} \rightarrow \{M^{n+}\}_x[CpW(CO)_3]^- + \{OH^-\}$$

where $\{M^{n+}\}_x\{O^{2-}\}$ represents a surface acid–base site and $\{M^{n+}\}_x[CpW(CO)_3]^-$ represents the resultant surface-bound anion. As demonstrated below, the number of cations x associated with each surface-bound anion can be 1 or 2, and the structure of the $[CpW(CO)_3]$ moiety is influenced strongly by interactions with $\{M^{n+}\}$.

(22) Anderson, P. J.; Horlock, R. F.; Oliver, J. F. *Trans. Faraday Soc.* **1965**, *61*, 2754.
(23) Deane, A. M.; Griffiths, D. L.; Lewis, I. A.; Winter, J. A.; Tench, A. J. *J. Chem. Soc., Faraday Trans. 1* **1975**, *71*, 1005.

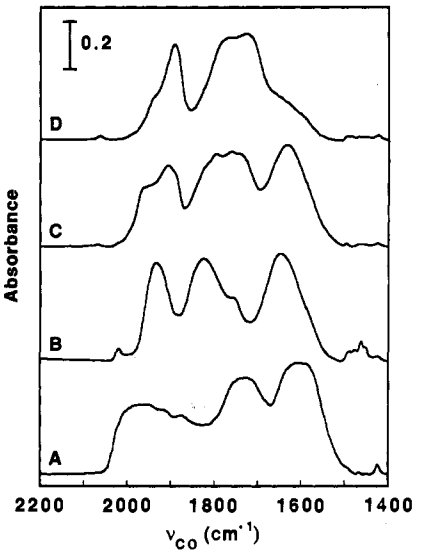

Figure 1. Infrared spectra of surface species derived by adsorption of $[HCpW(CO)_3]$ from toluene solution on (A) γ-Al_2O_3 pretreated at 800 °C *in vacuo*; (B) γ-Al_2O_3 pretreated at 400 °C *in vacuo*; (C) K/Al_2O_3, incorporating 1.6 K/nm^2, pretreated at 800 °C *in vacuo*; and (D) K/Al_2O_3, incorporating 7.2 K/nm^2, pretreated at 800 °C *in vacuo*.

Table 2. Infrared Data of Surface-Bound $[CpW(CO)_3]^-$ and Model Compounds

species	support/ solvent	ν_{CO} (cm^{-1})			reference
I[a]	γ-Al_2O_3	1980	1740	1610	this work
I[b]	γ-Al_2O_3	1987	1738	1625	this work
$[(AlMe_2)CpW(CO)_3]_2$	mch[c]	1981	1685	1650	25
II	γ-Al_2O_3	1937	1826	1650	this work
$Al[(CpW(CO)_3]_3$	THF	1942	1854	1591	26, 27
$NBu_4[CpW(CO)_3{\cdot}AlPh_3]$	CH_2Cl_2	1922	1825	1600	28
III	MgO	1887	1780	1705	this work
$Mg[CpMo(CO)_3]_2$	THF	1912	1815	1680	29
IV	MgO	1926	1750	1655	this work
V	K/Al_2O_3	1892	1769	1727	this work
$K[CpW(CO)_3]$	THF	1894	1784	1748	30

[a] $[HCpW(CO)_3]$ adsorption from solution. [b] Adsorption of $[HCpW(CO)_3]$ vapor. [c] Methylcyclohexane.

Characterization of Surface-Bound Anions by Infrared Spectroscopy. The ν_{CO} infrared spectrum of surface-bound $[CpW(CO)_3]^-$ on γ-Al_2O_3 pretreated at 800 °C *in vacuo* (Figure 1A) contains two low-frequency bands and a high-frequency band, which are assigned to species I (Table 2). A three-band pattern is expected for a $[CpW(CO)_3]$ moiety having C_s symmetry. From the infrared band frequencies, we infer that I has a structure containing two $WCO\cdots\{Al^{3+}\}$ isobridging ligands. The two ν_{CO} bands with frequencies less than the E mode frequency of C_{3v} $[CpW(CO)_3]^-$ are assigned to the symmetric and antisymmetric stretching vibrations of a pair of Σ–CO– ligands. A 90-cm^{-1} blue shift relative to the A_1 mode frequency of the C_{3v} anion is observed for the remaining band. This stretching mode is believed to involve principally the terminal CO ligand, and a substantial

(24) Shoulders at 2025 and 1915 cm^{-1} are assigned to molecularly adsorbed $[HCpW(CO)_3]$, and the small band at 1875 cm^{-1} is assigned to weakly perturbed $[CpW(CO)_3]^-$.
(25) Conway, A. J.; Gainsford, G. J.; Schrieke, R. R.; Smith, J. D. *J. Chem. Soc. Dalton Trans.* **1975**, 2499.
(26) Petersen, R. B.; Stezowski, J. J.; Wan, C.; Burlitch, J. M.; Hughes, R. E. *J. Am. Chem. Soc.* **1971**, *93*, 3532.
(27) The ν_{CO} spectrum of $(THF)_3Al[CpW(CO)_3]_3$ contains four low-frequency bands (1655 w, 1591 vs, 1567 s, and 1548 w cm^{-1}) which apparently arise from intramolecular vibrational coupling between Σ–CO– ligands.
(28) (a) Burlitch, J. M.; Petersen, R. B. *J. Organomet. Chem.* **1970**, *24*, C65. (b) Burlitch, J. M.; Leonowicz, M. E.; Petersen, R. B.; Hughes, R. E. *Inorg. Chem.* **1979**, *18*, 1097.
(29) McVicker, G. B. *Inorg. Chem.* **1975**, *14*, 2087.
(30) Darensbourg, M. Y.; Jimenez, P.; Sackett, J. R.; Hanckel, J. M.; Kump, R. L. *J. Am. Chem. Soc.* **1982**, *104*, 1521.

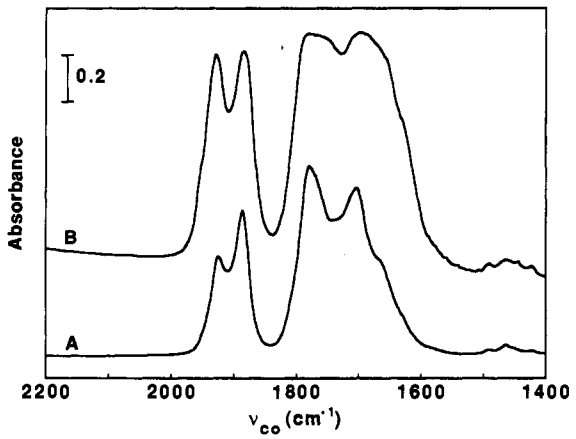

Figure 2. Infrared spectra of surface species derived by adsorption of [HCpW(CO)$_3$] from toluene solution on MgO: (A) 0.65 complexes/nm^2; (B) 1.3 complexes/nm^2.

blue shift is expected as a consequence of electron withdrawal by the Σ–CO– ligands. The pattern of ν_{CO} bands agrees well with that of [(AlMe$_2$)CpW(CO)$_3$]$_2$ (Table 2), a crystallographically defined molecule in which each [CpW(CO)$_3$] moiety bridges the two Al centers via two Σ–CO– ligands.

Adsorption of [HCpW(CO)$_3$] on partially dehydroxylated γ-Al$_2$O$_3$ gave somewhat inconsistent results, and often a mixture of [CpW(CO)$_3$]$^-$ surface species was obtained. The mixtures consisted of species **I** and species **II**; the infrared bands of the latter (Table 2) are assigned on the basis of the infrared spectrum in Figure 1B.[31] In contrast to the infrared spectrum of **I** (Figure 1A), that of **II** contains only one low-frequency ν_{CO} band which can be associated with a Σ–CO– ligand. On the basis of this observation and good agreement between the infrared spectrum of **II** and those of the isocarbonyl compounds Al[CpW(CO)$_3$]$_3$ and NBu$_4$[CpW(CO)$_3$·AlPh$_3$] in solution (Table 2), we conclude that **II** has a structure containing only one WCO···{Al^{3+}} isobridging ligand.

The ν_{CO} infrared spectrum of [CpW(CO)$_3$]$^-$ on MgO pretreated at 800 °C *in vacuo* (Figure 2A) is more complex than expected for a single surface-bound species. The six principal absorptions, a pair of bands at higher frequency, two strong bands at lower frequency, and low-frequency shoulders on the latter bands, are assigned to two surface-bound [CpW(CO)$_3$]$^-$ species. The three more intense bands are assigned to species **III**, and the remaining high-frequency band and the shoulders are assigned to species **IV** (Table 2). Comparison of the infrared spectra of [CpW(CO)$_3$]$^-$ on MgO at 0.65 and 1.3 W complexes/nm^2 (Figure 2) suggests that formation of **IV** is favored at higher coverage.

A structure containing one WCO···{Mg^{2+}} isobridging ligand is proposed for **III**, by analogy to the ion-pairing interaction in (py)$_4$Mg[CpMo(CO)$_3$]$_2$.[32] Only one ν_{CO} band which can be associated with a Σ–CO– ligand is observed, and the remaining bands are nearly coincident with the A$_1$ and E mode frequencies of the unperturbed anion. The infrared spectrum of **IV** is distinguished from that of **III** primarily by a 39-cm^{-1} blue shift of the highest ν_{CO} frequency and a 50-cm^{-1} red shift of the lowest ν_{CO} frequency. Because the bands are broad and overlapping, it is difficult to determine precisely the frequency of the middle band, but it appears to be shifted ~20 cm^{-1} lower relative to the E mode of C_{3v} [CpW(CO)$_3$]$^-$. These observations are consistent with a surface structure containing two WCO···{Mg^{2+}} isobridging ligands.

The ν_{CO} infrared spectrum of [CpW(CO)$_3$]$^-$ on K/Al$_2$O$_3$ incorporating 1.6 K cations/nm^2 (Figure 1C) contains at least six bands, consistent with a mixture of **II** and {K$^+$}[CpW(CO)$_3$]$^-$ surface species. In contrast, only three broad bands are prominent in the infrared spectrum of [CpW(CO)$_3$]$^-$ on K/Al$_2$O$_3$ incorporating 7.2 K cations/nm^2 (Figure 1D). This spectrum is assigned to **V**, a surface structure containing one WCO···{K$^+$} isobridging ligand. This assignment is based on the weak splitting of the low-frequency bands and good agreement between the infrared spectrum of **V** and that of its molecular analogue, K[CpW(CO)$_3$] in THF (Table 2).

Force Constant Calculations. Approximate CO stretching force constants of surface-bound [CpW(CO)$_3$]$^-$ were estimated from the observed ν_{CO} frequencies using an energy-factored force field[33] and idealized C_s symmetry of the carbonyl ligands.[34] Infrared band assignments made on the basis of proposed structures of the surface ion adducts were used (Table 3). Species **II**, **III**, and **V** contain one Σ–CO– ligand, whereas **I** and **IV** contain two Σ–CO– ligands. The force constants of the Σ–CO– and terminal CO ligands are designated k_{iso} and k_t, respectively. The models also contain two interaction force constants: k_i, describing vibrational coupling between symmetry-equivalent CO groups, and k_i', describing vibrational coupling between symmetry-inequivalent CO groups. Consequently, the resultant secular determinant contains four unknown parameters. To allow calculation of CO force constants using only the three observed frequencies, k_i' was assumed equal to 0.54 mdyn/Å, the value found by Darensbourg *et al.* for ^{13}CO-enriched Na$^+$[CpW(CO)$_2$(Σ–CO–)]$^-$ in solution.[30] Values of the ratio k_i/k_i' were calculated to provide an *ad hoc* estimate of the validity of the solutions. The results are given in Table 3. With the exception of **I**, the calculated k_i/k_i' ratios for the surface species are equivalent to or only slightly greater than 1.25, the ratio found for Na$^+$[CpW(CO)$_2$(Σ–CO–)]$^-$. The larger k_i/k_i' ratio calculated for **I** may indicate greater vibrational coupling between the two symmetry-equivalent Σ–CO– ligands. The k_t values characterizing **I** and **IV** are significantly greater than for **II** and **III**, respectively. For each species, a weighted-average CO force constant was calculated from the observed ν_{CO} frequencies; this value is *independent* of the proposed band assignments but can be computed as $(1/3)(k_{iso} + 2\,k_t)$ for species containing one Σ–CO– ligand and as $(1/3)(k_t + 2\,k_{iso})$ for species containing two Σ–CO– ligands.

Characterization of Surface-Bound Anions by EXAFS Spectroscopy. The EXAFS spectra characterizing samples prepared by adsorption of [HCpW(CO)$_3$] from toluene solution onto highly dehydroxylated MgO, γ–Al$_2$O$_3$, and K/Al$_2$O$_3$ were Fourier-filtered to isolate the first-shell contributions. The resultant spectra (Figure 3A–C) were analyzed to determine the average structures of the surface-bound [CpW(CO)$_3$]$^-$ complexes. The W–C phase-corrected Fourier transforms contain three peaks arising from C and O backscatterers (Figure 3D–F). The peak near 2.0 Å is assigned to the C atoms of the CO ligands and is denoted by C*; the peak near 2.4 Å is assigned to the C atoms of the Cp ligand; and the peak near 3.0 Å is assigned to the O atoms of the CO ligands and is denoted by O*. The O* peak is accentuated and exhibits a phase shift of nearly π radians, owing to multiple scattering in the nearly linear W–C–O linkage.[35] In the EXAFS analysis, the coordination numbers of the three types of backscatterers were fixed at the values expected by stoichiometry, thereby reducing the number of free parameters. The results of three-component fitting (k^2 weighting, $3.5 \le k \le 12.5$ Å^{-1}) of the EXAFS spectra are given in Table 4; EXAFS functions calculated by using these parameters are compared with the data in Figure 3.

(31) A weak band at 2022 cm^{-1} and a shoulder at 1920 cm^{-1} are assigned to adsorbed hydride, and a band at 1750 cm^{-1} is associated with weakly perturbed [CpW(CO)$_3$]$^-$.

(32) Ulmer, S. W.; Skarstad, P. M.; Burlitch, J. M.; Hughes, R. E. *J. Am. Chem. Soc.* **1973**, *95*, 4469.

(33) Cotton, F. A.; Kralhanzel, C. S. *J. Am. Chem. Soc.* **1962**, *84*, 4432.

(34) Species **I** and **IV** may not have C_s symmetry, *i.e.*, the Σ–CO– ligands might not be rigorously symmetry-equivalent, but the assumption of C_s symmetry allowed for reasonable estimates of CO stretching force constants.

(35) (a) van't Blik, H. F. J.; van Zon, J. B. A. D.; Huizinga, T.; Vis, J. C.; Koningsberger, D. C.; Prins, R. *J. Am. Chem. Soc.* **1985**, *107*, 3139. (b) Duivenvoorden, F. B. M.; Koningsberger, D. C.; Uh, Y.-S.; Gates, B. C. *J. Am. Chem. Soc.* **1986**, *108*, 6254.

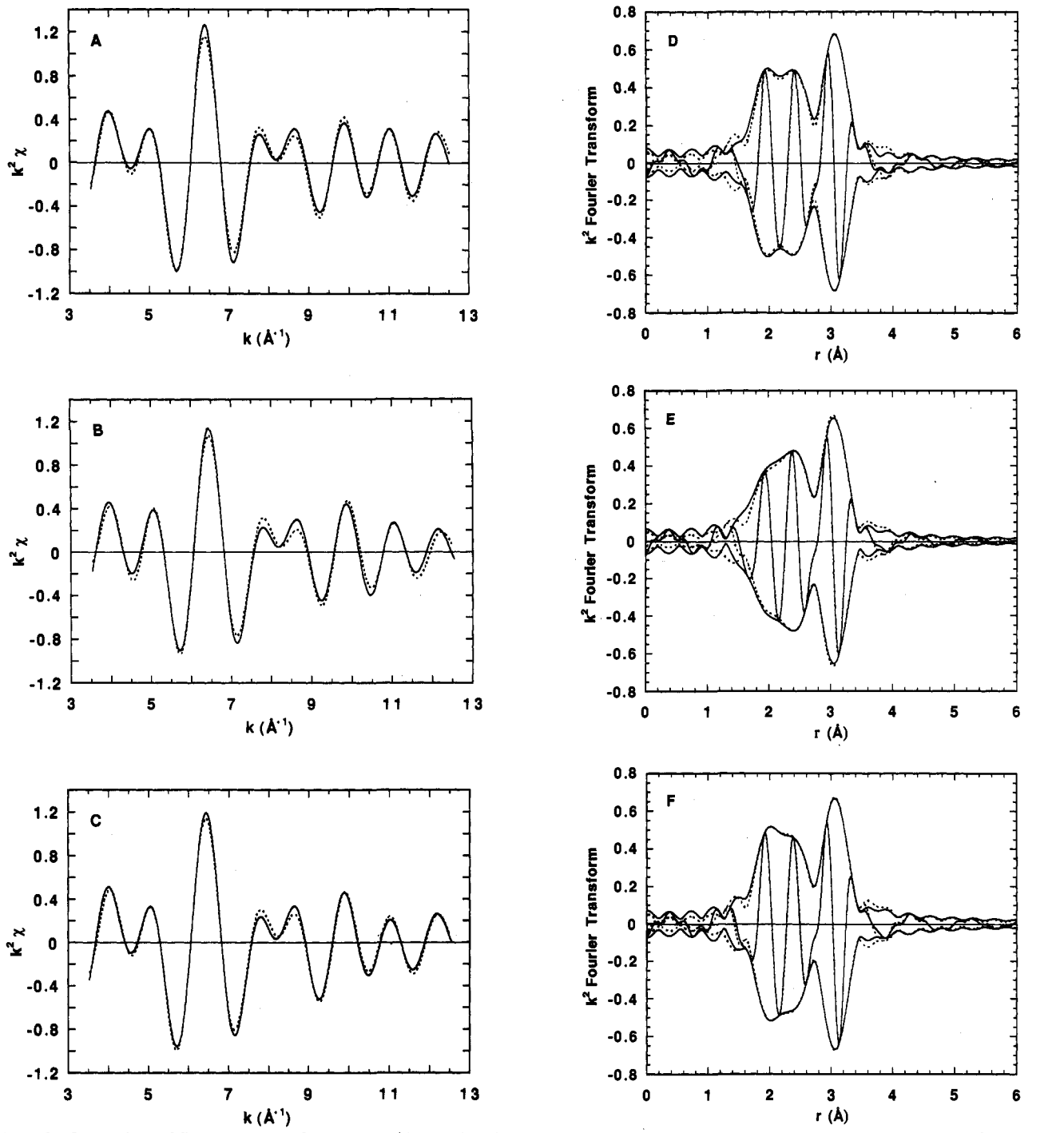

Figure 3. Comparison of first-shell EXAFS spectra (solid curves) and calculated best fits (dashed curves) in k space and r space: (A) k^2-weighted EXAFS of surface species derived by adsorption of $[HCpW(CO)_3]$ on MgO; (B) k^2-weighted EXAFS of surface species derived by adsorption of $[HCpW(CO)_3]$ on γ-Al_2O_3; (C) k^2-weighted EXAFS of surface species derived by adsorption of $[HCpW(CO)_3]$ on K/Al_2O_3; (D) W–C phase-corrected Fourier transform associated with A; (E) W–C phase-corrected Fourier transform associated with B; (F) W–C phase-corrected Fourier transform associated with C.

Table 3. Approximate CO Stretching Force Constants of Surface-Bound $[CpW(CO)_3]^-$

species	proposed structure	ν_{CO} (cm^{-1})			force constants (mdyn/Å)			
		A′	A′	A″	k_{ave}	k_{iso}	k_t	k_i/k_i'
I	$\{Al^{3+}\}_2[CpW(CO)(\Sigma\text{–}CO\text{–})_2]^-$	1980	1740	1610	12.8	11.4	15.7	1.78
II	$\{Al^{3+}\}[CpW(CO)_2(\Sigma\text{–}CO\text{–})]^-$	1937	1650	1826	13.2	11.1	14.2	1.43
III	$\{Mg^{2+}\}[CpW(CO)_2(\Sigma\text{–}CO\text{–})]^-$	1887	1705	1780	13.0	12.0	13.5	1.24
IV	$\{Mg^{2+}\}_2[CpW(CO)(\Sigma\text{–}CO\text{–})_2]^-$	1926	1750	1655	12.8	11.8	14.7	1.44
V	$\{K^+\}[CpW(CO)_2(\Sigma\text{–}CO\text{–})]^-$	1892	1727	1769	13.0	12.3	13.4	1.43

To assess the reliability of the average interatomic distances obtained by the analysis procedure, the EXAFS spectrum of $[CpW(CO)_3]_2$ crystals dispersed in boron nitride was measured and analyzed. In the EXAFS analysis, the W–W contribution was simulated using the crystallographically determined bond distance. In Table 5, the fitting results are compared with selected interatomic distances from the X-ray crystal structure of the dimer.[36] Excellent agreement is found for the W–C* and W–C

Table 4. Structures of Surface Species Derived by Adsorption of $[HCpW(CO)_3]$, as Determined by EXAFS Spectroscopy

species	back-scatterer[a]	N	r (Å)[b]	$\Delta\sigma^2 \times 10^3$ (Å^2)[c]	ΔE_0 (eV)
$[CpW(CO)_3]^-$ on K/Al_2O_3	C*	3	1.93	0.34	0.0
	C	5	2.36	1.3	–0.9
	O*	3	3.14	–0.12	–4.8
$[CpW(CO)_3]^-$ on MgO	C*	3	1.92	0.51	3.0
	C	5	2.37	1.0	0.3
	O*	3	3.14	–0.36	–3.4
$[CpW(CO)_3]^-$ on γ-Al_2O_3	C*	3	1.93	2.0	2.4
	C	5	2.36	0.79	–1.4
	O*	3	3.14	0.17	–4.7

[a] C* and O* are the carbonyl C and carbonyl O backscatterers, respectively. C is the cyclopentadienyl C backscatterer. [b] Estimated uncertainty in r: ±0.02 Å. [c] Estimated uncertainty in $\Delta\sigma^2$: ±0.5 × 10^{-3} Å^2.

Table 5. Structure of Tungsten Cyclopentadienyltricarbonyl Dimer as Determined by EXAFS Spectroscopy: Comparison with Crystal Structure Data

backscatterer	N	R (Å)[a]	r (Å)[b]	$\Delta\sigma^2 \times 10^3$ (Å^2)[c]	ΔE_0 (eV)
C*	3	1.976	1.98	–0.43	3.0
C	5	2.342	2.35	1.5	1.7
O*	3	3.125	3.16	–0.11	–3.2
W	1	3.222		0.46	–4.6

[a] Average interatomic distances from X-ray crystal structure determination.[36] [b] Average interatomic distances from EXAFS analysis; W–W distance was not estimated but was simulated using the crystallographically determined bond distance. Estimated uncertainty in r: ±0.02 Å. [c] Estimated uncertainty in $\Delta\sigma^2$: ±0.5 × 10^{-3} Å^2.

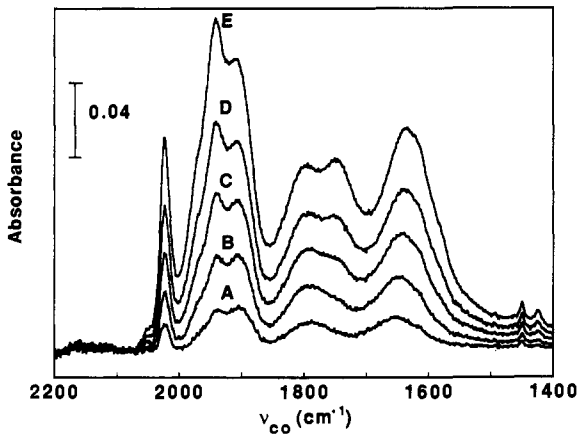

Figure 4. Infrared spectra of surface species derived by adsorption of $[HCpW(CO)_3]$ vapor on γ-Al_2O_3 pretreated at 800 °C *in vacuo*. Spectra were recorded with sample *in vacuo* after cumulative exposure times of (A) 5 min; (B) 10 min; (C) 15 min; (D) 20 min; and (E) 25 min.

distances, but the W–O* distance is overestimated by 0.035 Å. There are two likely reasons: (1) differences in W–C–O multiple-scattering effects between the dimer and the $W(CO)_6$ reference compound and (2) interference of the W–O* and W–W contributions to the dimer spectrum. The first factor is expected to be small and difficult to quantify, as the W–C–O angles in both compounds are approximately 180°. The second factor is unique to the dimer structure; there is no evidence of W–W contributions to the EXAFS spectra of the surface species.

Adsorption of $[HCpW(CO)_3]$ Vapor on γ-Al_2O_3. Infrared difference spectra recorded *in vacuo* after exposure of highly dehydroxylated γ-Al_2O_3 to $[HCpW(CO)_3]$ vapor (Figure 4) indicate that both molecular adsorption and deprotonation occur at 25 °C. Strong ν_{CO} bands at 2025 and 1909 cm^{-1} are assigned to molecularly adsorbed hydride,[37] and the remaining bands are assigned to surface-bound $[CpW(CO)_3]^-$ (species **I** and **II**). The

(36) Adams, R. D.; Collins, D. M.; Cotton, F. A. *Inorg. Chem.* **1974**, *13*, 1086.

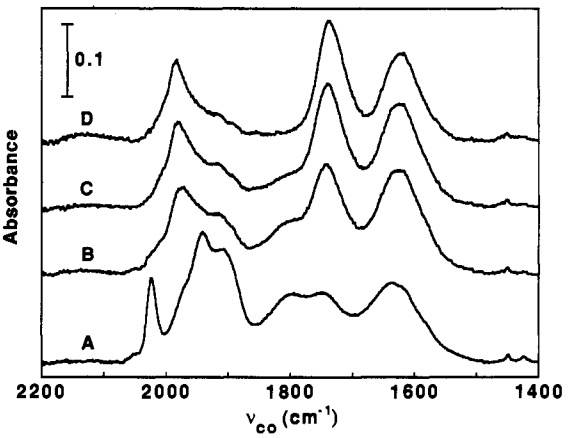

Figure 5. Infrared spectra of surface species derived by adsorption of $[HCpW(CO)_3]$ vapor on γ-Al_2O_3, after heating *in vacuo* at (A) 30 °C; (B) 50 °C; (C) 70 °C; and (D) 100 °C.

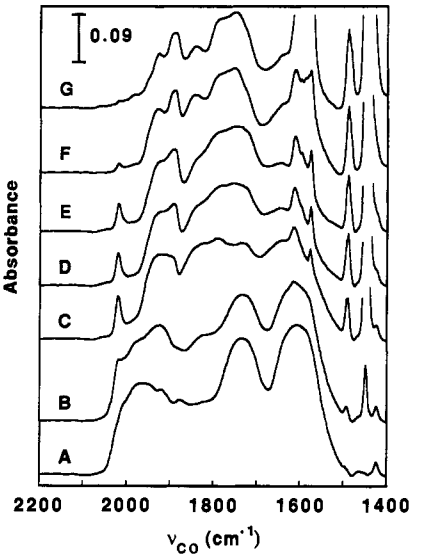

Figure 6. Infrared spectra illustrating the effects of pyridine adsorption on $\{Al^{3+}\}_2[CpW(CO)(\Sigma\text{–}CO\text{–})_2]^-$ adducts on γ-Al_2O_3: (A) initial; (B) 0.02 Torr of pyridine; (C) 0.1 Torr; (D) 0.3 Torr; (E) 0.6 Torr; (F) 1.2 Torr; and (G) 4.4 Torr.

spectrum observed after the initial dose of $[HCpW(CO)_3]$ vapor (Figure 4A) evidences hydride adsorption and formation of **II**. Species **I** forms only slowly and after several exposures to hydride vapor, as indicated by the growth of a band at 1740 cm^{-1} and shoulders at 1990 and 1625 cm^{-1} (Figure 4C-E). Heating the wafer to 50 °C *in vacuo* resulted in substantial conversion of adsorbed hydride to **I**, as evidenced by nearly complete elimination of $[HCpW(CO)_3]$ ν_{CO} bands and concomitant increases in the ν_{CO} bands of **I** (Figure 5B). Heating to 70 °C (Figure 5C) and 100 °C (Figure 5D) *in vacuo* resulted in gradual conversion of residual **II** to **I**.

Adsorption of Pyridine with $[CpW(CO)_3]^-$ on γ-Al_2O_3. The interaction of adsorbed pyridine with **I** on γ-Al_2O_3 was investigated by infrared spectroscopy. Exposure of the surface to 0.02 Torr of pyridine vapor resulted in formation of **II** and $[HCpW(CO)_3]$, as evidenced by the increased intensities of bands assigned to these species and decreased intensities of bands assigned to **I** (Figure 6B). Increasing the pyridine pressure to 0.1 Torr eliminated **I**, as evidenced by the disappearance of the band at 1980 cm^{-1} (Figure 6C). The remaining bands are consistent with the presence of $[HCpW(CO)_3]$, **II**, and C_{3v} $[CpW(CO)_3]^-$.

(37) In solution, $[HCpW(CO)_3]$ has ν_{CO} bands at 2020 s and 1925 vs cm^{-1}; the slight shift of the bands upon adsorption suggests a weak chemical interaction.

The bands at 1616 and 1576 cm^{-1} are assigned to the 8a and 8b modes, respectively, of pyridine N coordinated to $\{Al^{3+}\}$.[38] The bands at 1491 and 1448 cm^{-1} are assigned to the 19a and 19b modes of pyridine and are insensitive to N coordination. The ν_{8a} band at 1616 cm^{-1} appears to saturate at a pyridine pressure of 0.6 Torr (Figure 6E); further increases in the 1576-cm^{-1} band are attributed to a contribution from the 8a mode of physisorbed pyridine at 1579 cm^{-1}. Above 0.6 Torr (Figure 6F,G) the bands of C_{3v} $[CpW(CO)_3]^-$ become the predominant ν_{CO} bands. The observed loss of integrated ν_{CO} intensity during the experiment is believed to result from sublimation of $[HCpW(CO)_3]$ *in vacuo*.

Discussion

Deprotonation of $[HCpW(CO)_3]$ on Basic Metal Oxides. The deprotonation of hydrido carbonyls on basic metal oxide surfaces is a general approach to preparation of surface-bound metal carbonyl anions.[4] Hydrido carbonyls are weak Brønsted acids in solution;[39] in the gas phase, they are strong acids, owing to the ability of π-acid CO ligands to delocalize electronic charge.[40] We anticipated that $[HCpW(CO)_3]$ (pK_a = 9.0 (methanol)) would be readily deprotonated to form surface-bound $[CpW(CO)_3]^-$ on MgO and basic K/Al_2O_3 but that deprotonation might be more difficult on highly dehydroxylated γ-Al_2O_3.[41] Organic Brønsted acids chemisorb dissociatively on highly dehydroxylated MgO via deprotonation at surface acid–base pair sites $\{Mg^{2+}\}\{O^{2-}\}$. This process results in the formation of a surface hydroxyl group $\{OH^-\}$ and a conjugate base anion (B^-) stabilized by bonding with a coordinatively unsaturated Mg cation.[42,43] The ion adduct $\{Mg^{2+}\}B^-$ is the surface analogue of the solution chemist's contact ion pair.[11] Although γ-Al_2O_3 does not exhibit the strong basicity characteristic of MgO, a similar chemistry has been reported for the dissociative adsorption of alcohols on dehydroxylated γ-Al_2O_3.[44]

The experimental results demonstrate that $[HCpW(CO)_3]$ is chemisorbed from solution by deprotonation on each basic metal oxide; only on γ-Al_2O_3 was there any evidence of molecularly adsorbed $[HCpW(CO)_3]$. Similar surface species are produced by adsorption of $[HCpW(CO)_3]$ vapor on γ-Al_2O_3, as evidenced by *in situ* infrared spectra. This result indicates that the toluene solvent did not play a significant role in the surface chemistry.

Structures of Surface-Bound $[CpW(CO)_3]^-$. Selected bond lengths in the surface-bound $[CpW(CO)_3]^-$ complexes, which were determined by EXAFS spectroscopy, are compared in Table 6 with those found by X-ray crystallography of cyclopentadienyltricarbonyltungstate(−1) model compounds.[45] In the surface-bound complexes, the average W–C bond distance associated with the Cp ligand is in excellent agreement with that found in $(THF)_3Al[CpW(CO)_3]_3$ and is consistent with pentahapto coordination of the ring. The W–C* and C–O bond lengths are in good agreement with the average distances found in the model compounds.

Table 6. Bond Lengths (Å) in Surface-Bound $[CpW(CO)_3]^-$ and Model Compounds

species	W–C[a]	W–C[b]	C–O[c]	reference
I	2.36	1.93	1.21	this work
III and IV[d]	2.37	1.92	1.22	this work
V	2.36	1.93	1.21	this work
$(THF)_3Al[CpW(CO)_3]_3$	2.36[e]	1.92	1.19	26
$[(AlMe_2)CpW(CO)_3]_2$	2.34[e]	1.89	1.21	25

[a] Average W–C distance to Cp ligand. Estimated uncertainty in determination by EXAFS spectroscopy (this work): ±0.02 Å. [b] Average W–carbonyl carbon bond length. Estimated uncertainty in determination by EXAFS spectroscopy (this work): ±0.02 Å. [c] Average C–O bond length. Estimated uncertainty in determination by EXAFS spectroscopy (this work): ±0.04 Å. [d] Average structure including contributions from III and IV. [e] Estimated from reported perpendicular distance to centroid of Cp ring.

In isocarbonyl compounds, metal–carbon bonds are substantially shorter and C–O bonds longer for Σ–CO– ligands than for terminal carbonyl ligands.[25,26,32] From EXAFS data, it is not possible to determine individual carbonyl W–C* bond distances, but the Debye–Waller correction ($\Delta\sigma^2$) provides an estimate of disorder within the W–C* shell.[46] For surface-bound $[CpW(CO)_3]^-$, the $\Delta\sigma^2$ values of the W–C* shells are significantly larger (Table 4) than that found by fitting the EXAFS spectrum of crystalline $[CpW(CO)_3]_2$ (Table 5). Moreover, the disorder in W–C* bond distances increases with the electrostatic potential (charge-to-radius ratio) of the surface counter cation, i.e., in the order $\{K^+\} < \{Mg^{2+}\} < \{Al^{3+}\}$. These observations cannot be attributed to the effects of temperature nor to overall static disorder in the surface structures, as the $\Delta\sigma^2$ values of the W–C and W–O* shells are in close agreement with the values observed for the corresponding shells in the dimer. Instead, these results are diagnostic of Σ–CO– bonding of one or two CO ligands in surface-bound $[CpW(CO)_3]^-$, consistent with the infrared spectra.

The ν_{CO} infrared spectrum $[CpW(CO)_3]^-$ on each metal oxide is unique, owing to the interactions of carbonyl O atoms with surface counter cations.[47] In solution, this acid–base interaction typically involves only one carbonyl ligand of each $[CpW(CO)_3]$ moiety, as observed in the alkali metal, Mg, and Al salts. For surface-bound $[CpW(CO)_3]$-, two types of isocarbonyl structures, those containing one and those containing two Σ–CO– ligands per complex, are observed.

The infrared band assignments for C_{3v} $[CpW(CO)_3]^-$ and for each type of ion adduct on γ-Al_2O_3 are illustrated in Figure 7. O coordination of one carbonyl ligand results in C_s symmetry of the $[CpW(CO)_3]$ moiety and in three infrared-active ν_{CO} modes: two A′ and A″ (Figure 7B). The A'_{iso} mode, which involves primarily the CO stretch of the Σ–CO– ligand, occurs at a frequency less than the E mode of unperturbed C_{3v} $[CpW(CO)_3]^-$. As suggested by its lower ν_{CO} frequency, the π acidity of the Σ–CO– ligand is enhanced, and the remaining terminal carbonyls share less W electron density. Consequently, the A′ and A″ bands are at frequencies slightly higher than the A_1 and E mode frequencies, respectively, of C_{3v} $[CpW(CO)_3]^-$. For the ion adducts containing two Σ–CO– ligands, the $[CpW(CO)_3]$ moiety also will have C_s symmetry, provided that the two isobridging ligands are equivalent.[34] In C_s symmetry (Figure 7C), the two bands that appear at frequencies less than the E mode frequency of C_{3v} $[CpW(CO)_3]^-$ (A'_{iso} and A''_{iso}) can be envisioned to arise from the symmetric and antisymmetric CO stretching vibrations

(38) (a) Scokart, P. O.; Declerck, F. D.; Sempels, R. E.; Rouxhet, P. G. *J. Chem. Soc., Faraday Trans. 1* **1977**, *73*, 359. (b) Scokart, P. O.; Rouxhet, P. G. *J. Colloid Interface Sci.* **1982**, *86*, 96.

(39) Pearson, R. G. *Chem. Rev.* **1985**, *85*, 41.

(40) Miller, A. E. S.; Beauchamp, J. L. *J. Am. Chem. Soc.* **1991**, *113*, 8765.

(41) Kirlin, P. S.; DeThomas, F. A.; Bailey, J. W.; Gold, H. S.; Dybowski, C.; Gates, B. C. *J. Phys. Chem.* **1986**, *90*, 4882.

(42) Garrone, E.; Stone, F. S. *Proc. Int. Congr. Catal. 8th* **1984**, III-441.

(43) (a) Spitz, R. N.; Barton, J. E.; Barteau, M. A.; Staley, R. H.; Sleight, A. W. *J. Phys. Chem.* **1986**, *90*, 4067. (b) Peng, X. D.; Barteau, M. A. *Langmuir* **1991**, *7*, 1426.

(44) (a) Jeziorowski, H.; Knözinger, H.; Meye, W.; Müller, H. D. *J. Chem. Soc. Faraday Trans. 1* **1973**, *69*, 1744. (b) Knözinger, H. In *The Hydrogen Bond*; Schuster, P., Zundel, G., Sandorfy, C., Eds.; North Holland: Amsterdam, 1976. (c) Knözinger, H.; Stübner, B. *J. Phys. Chem.* **1978**, *82*, 1526.

(45) The EXAFS spectroscopy results reveal the average structure of W surface species on each metal oxide. Consequently, the distances reported for $[CpW(CO)_3]^-$ on γ-Al_2O_3 and K/Al_2O_3 are characteristic of species I and V, respectively, but the distances reported for $[CpW(CO)_3]^-$ on MgO represent a composite structure, including both species III and IV.

(46) The Debye–Waller correction is a measure of the mean square variation in interatomic distances *relative* to the reference compound. As there are static and thermal contributions to disorder, spectra of the $[W(CO)_6]$ reference compound and the samples were recorded at the same temperature.

(47) The $[CpW(CO)_3]$ anion can be regarded as exhibiting hard base (carbonyl O) and soft base (W) sites for interaction with cations. For $[CpW(CO)_3]^-$ in nonpolar solvents, the contact interaction with hard metal cations involves a basic carbonyl O, forming an isocarbonyl bridge. Soft counter cations having unfilled d orbitals, such as Zn, Cd, and Hg, typically bond directly with the tungsten center.

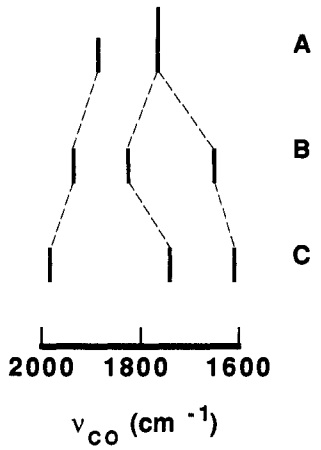

Figure 7. Infrared band assignments for C_{3v} $[CpW(CO)_3]^-$ (A) and for the $[CpW(CO)_2(\Sigma\text{–}CO\text{–})]^-$ (B) and $[CpW(CO)(\Sigma\text{–}CO\text{–})_2]^-$ (C) ion adducts on γ-Al_2O_3.

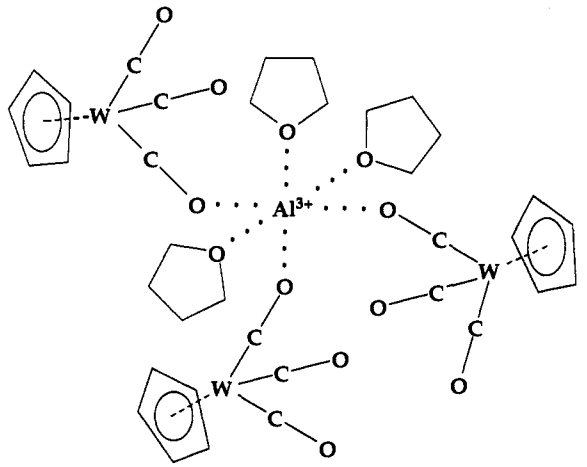

Figure 8. Molecular structure of $(THF)_3Al[CpW(CO)_3]_3$.[26]

of the two Σ–CO– ligands. The remaining A′ mode is associated primarily with vibration of the terminal CO ligand. This band exhibits a substantial blue shift relative to the A_1 band of C_{3v} $[CpW(CO)_3]^-$, owing to electron withdrawal from W by the two strongly π-acidic Σ–CO– ligands.

$\{M^{n+}\}[CpW(CO)_2(\Sigma\text{–}CO\text{–})]^-$ (M = Al, Mg, K) Adducts (II, III, and V). $\{M^{n+}\}[CpW(CO)_2(\Sigma\text{–}CO\text{–})]^-$ adducts are formed on each metal oxide surface. The solid-state structure of $(THF)_3Al[CpW(CO)_3]_3$ (Figure 8) provides a basis for understanding the surface structures. Coordination of three $[CpW(CO)_3]$ moieties to Al via carbonyl O atoms is observed; the Al–O bonds are short (1.83 Å), and the C–O–Al angles range from 140.4 to 162.9°.[26] The characteristic deviation of the C–O–M angles from 180° reflects interaction of the cation with electrons in the CO σ and π* molecular orbitals. In the closely related structure of $(py)_4Mg[CpMo(CO)_3]_2$,[32] the metal-oxygen bonds are longer (2.05 Å), indicating that the bond strength depends markedly on the counter-cation electrostatic potential. As the interaction is localized at a single carbonyl O atom, the steric requirements are low, and formation of $\{M^{n+}\}[CpW(CO)_2(\Sigma\text{–}CO\text{–})]^-$ adducts is observed on partially dehydroxylated and highly dehydroxylated γ-Al_2O_3 surfaces. The O atom of the Σ–CO– ligand can be envisaged as completing the coordination sphere of a $\{M^{n+}\}$ ion terminating the bulk metal oxide.

On K/Al_2O_3, $[CpW(CO)_3]^-$ proved to be a sensitive probe of surface composition. Owing to the large ionic radius of K^+, addition of $K(NO_3)$ to γ-Al_2O_3 and calcination at 800 °C is expected to result primarily in surface modification with little diffusion of K into the bulk.[48] Adsorption of $[HCpW(CO)_3]$ on γ-Al_2O_3 modified by addition of 1.6 K^+/nm^2 resulted in the formation of a mixture of $[CpW(CO)_2(\Sigma\text{–}CO\text{–})]^-$ species II and V, as evidenced by the ν_{CO} infrared spectrum in Figure 1C. Surface modification by 7.2 K^+/nm^2 strongly suppressed formation of the $\{Al^{3+}\}$ adduct II (Figure 1D). The required loading corresponds to approximately 0.5 K^+ per surface $\{O^{2-}\}$ on a completely dehydroxylated γ-$Al_2O_3(111)$ surface.[49,50] By using surface-bound $[CpW(CO)_3]^-$ as a probe, we conclude that at this loading the outermost layer of K/Al_2O_3 contains primarily $\{K^+\}$ ions. The above results are consistent with a report that addition of K_2CO_3 to γ-Al_2O_3 followed by calcination results in the formation of Al–OK surface groups.[51]

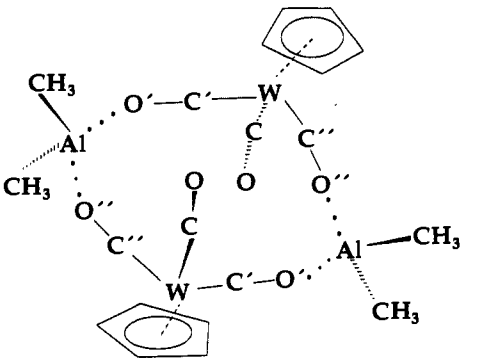

Figure 9. Molecular structure of $[(AlMe_2)CpW(CO)_3]_2$.[25]

$\{M^{n+}\}_2[CpW(CO)(\Sigma\text{–}CO\text{–})_2]^-$ (M = Al, Mg) Adducts (I and IV). On γ-Al_2O_3 and MgO, bis(isocarbonyl) ion adducts are formed. The solid-state structure of $[(AlMe_2)CpW(CO)_3]_2$ (Figure 9) provides a basis for understanding the surface structures. In this molecule, each $[CpW(CO)_3]$ moiety bridges two Al centers via Σ–CO– ligands. The $[CpW(CO)_3]$ bridges are asymmetric; one Σ–CO– ligand exhibits a typical C–O–Al angle of 149°, and the other is nearly linear (C–O–Al angle of 176°).[25] The geometry of the $[CpW(CO)_3]$ moiety and the relative positions of $\{M^{n+}\}$ counter cations on γ-Al_2O_3 and MgO surfaces favor formation of analogous $\{M^{n+}\}_2[CpW(CO)(\Sigma\text{–}CO\text{–})_2]^-$ structures. A bis(isocarbonyl) species interacting with a single counter cation might be accommodated at steps, kinks, and defect sites on a metal oxide surface, but these sites are expected to be too rare to account for the observed surface coverages (*vide infra*).

The models in Figures 10 and 11 illustrate that interaction of two $[CpW(CO)_3]^-$ carbonyl O atoms with two $\{M^{n+}\}$ ions can be accommodated on the ideal surface planes of γ-Al_2O_3 and MgO. In the model of I, the A layer of the γ-$Al_2O_3(111)$ face at slightly greater than 50% dehydroxylation is used. A triplet oxygen vacancy, as proposed by Knözinger and Ratnasamy,[50] which exposes two $\{Al^{3+}\}$ ions in tetrahedral interstices separated by 5.60 Å is suggested as a likely adsorption site for $[CpW(CO)_3]^-$. The Al–Al distance is shorter than the 6.39-Å Al–Al distance in $[(AlMe_2)CpW(CO)_3]_2$,[25] but the C–O–$\{Al^{3+}\}$ angle of 155° estimated for I at this site is typical of the C–O–M angles found in the model compounds. The ν_{CO} infrared spectrum of I is similar to that of $[(AlMe_2)CpW(CO)_3]_2$, but the splitting of the A'_{iso} and A''_{iso} bands of I is substantially larger for the surface species, indicating greater vibrational coupling between Σ–CO– ligands. *In situ* infrared spectroscopy of $[HCpW(CO)_3]$ vapor adsorption on γ-Al_2O_3 indicates that II is the initial product and that I forms slowly at 25 °C. Conversion of II to I is observed on heating at 70–100 °C *in vacuo*, suggesting that I is the more stable surface species and that diffusion to a favorable adsorption site might limit its rate of formation.

(48) Stork, W. H. J.; Pott, G. T. *J. Phys. Chem.* **1974**, *78*, 2496.
(49) Ideally, an γ-$Al_2O_3(111)$ surface is terminated by a cubic close-packed layer of hydroxyl groups; one-half of the O atoms are removed during dehydroxylation leaving anion vacancies and one-half monolayer of $\{O^{2-}\}$.
(50) Knözinger, H.; Ratnasamy, P. *Catal. Rev.-Sci. Eng.* **1978**, *17*, 31.
(51) Zaki, M. I.; Ballinger, T. H.; Yates, J. T., Jr. *J. Phys. Chem.* **1991**, *95*, 4028.
(52) Shriver, D. F. *J. Organomet. Chem.* **1975**, *94*, 259.

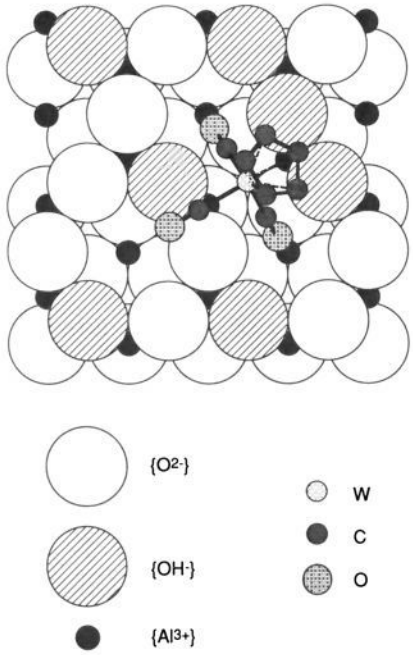

Figure 10. Model of $\{Al^{3+}\}_2[CpW(CO)(\Sigma\text{–}CO\text{–})_2]^-$ (**I**) on γ-Al_2O_3.

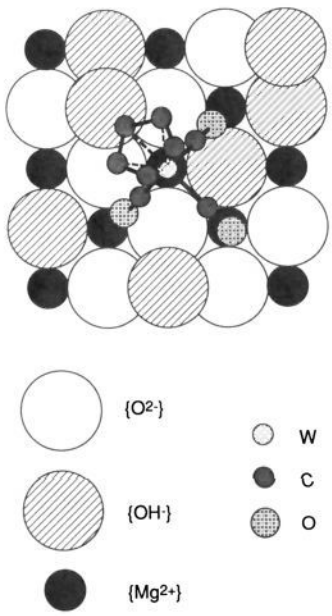

Figure 11. Model of $\{Mg^{2+}\}_2[CpW(CO)(\Sigma\text{–}CO\text{–})_2]^-$ (**IV**) on MgO.

In the model of **IV**, the MgO(100) plane at 70% dehydroxylation is used. Two $\{Mg^{2+}\}$ ions separated by 5.94 Å form the proposed adsorption site; the estimated C–O–$\{Mg^{2+}\}$ angle is 161°, which is within the range of observed C–O–M angles in the model compounds. As MgO powders are expected to expose predominantly the (100) surface plane, an estimate of the percentage of $\{Mg^{2+}\}\{O^{2-}\}$ sites involved in chemisorption of $[HCpW(CO)_3]$ can be made. The surface density of $\{Mg^{2+}\}\{O^{2-}\}$ pairs on MgO(100) is 11.3/nm²; therefore, at 0.65 complexes/nm², only 6% of the available $\{Mg^{2+}\}\{O^{2-}\}$ sites are used, which is nearly the expected percentage of four-coordinate and three-coordinate sites.[42] However, based on size and projected area, the maximum surface density of $[CpW(CO)_3]^-$ complexes is estimated as 2.7/nm²; consequently, 1.3 complexes/nm² corresponds to almost 50% of monolayer capacity. From this estimate, we conclude that on MgO the surface organometallic chemistry does not involve only steps, kinks, and defect sites. The observed preference of **IV** over **III** at higher coverage suggests that **III** forms preferentially at steps, kinks, and defect sites, which should be most reactive, and that **IV** forms primarily at five-coordinate sites on terraces.

Dissociation of $\{Al^{3+}\}_2[CpW(CO)(\Sigma\text{–}CO\text{–})_2]^-$ by Adsorbed Pyridine. The behavior of surface-bound $[CpW(CO)_3]^-$ on γ-Al_2O_3 in the presence of coadsorbed pyridine demonstrates that the ion adducts can be dissociated by strong donor molecules. At low pyridine pressures, N-coordinated pyridine (8a ring mode at 1615 cm⁻¹) displaces one Σ–CO– ligand of **I** from its interaction with $\{Al^{3+}\}$:

$$\{Al^{3+}\}_2[CpW(CO)(\Sigma\text{–}CO\text{–})_2]^- + py \rightarrow \{Al^{3+}\}[CpW(CO)_2(\Sigma\text{–}CO\text{–})]^- + py\cdot\{Al^{3+}\}$$

This parallels the conversion of $[(AlMe_2)CpW(CO)(\Sigma\text{–}CO\text{–})_2]_2$ to $AlMe_2[CpW(CO)_2(\Sigma\text{–}CO\text{–})]\cdot NMe_3$ in benzene solution by addition of trimethylamine.[25] At higher pyridine pressures, the $\{Al^{3+}\}$ sites are nearly saturated by pyridine and most of the surface-bound anions convert to the C_{3v} form:

$$\{Al^{3+}\}[CpW(CO)_2(\Sigma\text{–}CO\text{–})]^- + py \rightarrow [CpW(CO)_3]^- + py\cdot\{Al^{3+}\}$$

Analogous chemistry is observed in solution.[28]

Metal Carbonyl Anion–Lewis Acid Adducts on Surfaces. By comparing the CO stretching force constants of Σ–CO– ion adducts on metal oxides (Table 3) with those of their solution analogues, the nature of the electrostatic perturbations of $[CpW(CO)_3]^-$ by $\{M^{n+}\}$ can be elucidated. The weighted-average CO force constant (k_{ave}) of $[CpW(CO)_3]^-$ is a measure of electron transfer from W or CpW to the CO ligands.[30] The CO force constant of the carbonyl ligands in unperturbed $[CpW(CO)_3]^-$ (13.27 mdyn/Å) is used as a reference datum. As the k_{ave} values for each surface species are lower, this indicates that electron transfer is increased by O coordination of one or two carbonyl ligands by $\{M^{n+}\}$. The effects are larger than observed for contact ion pairs in solution,[30] and we infer that this electron-transfer mechanism is necessary to stabilize the $[CpW(CO)_3]$ anion on metal oxide surfaces. Interestingly, k_{ave} is relatively insensitive to the identity of the counter cation.

As evidenced by the k_{ave} values for the bis(isocarbonyl) species, two Σ–CO– ligands per complex are more effective than one in draining electronic charge from the metal center. This observation can be used to explain the greater stability of **I** on γ-Al_2O_3. As the $\{O^{2-}\}$ ions are expected to be less basic on γ-Al_2O_3 than on MgO or K/Al_2O_3, the energetics of deprotonation are more dependent on stabilization of the conjugate base anion by adduct formation. Consequently, surface-bound $[CpW(CO)_3]^-$ complexes on γ-Al_2O_3 are expected to adopt the more energetically favorable bis(isocarbonyl) structure, as observed during *in vacuo* annealing of the mixture of **I** and **II** derived by $[HCpW(CO)_3]$ vapor adsorption.

The carbonyl O atoms of metal carbonyl anions are hard base sites,[52] and their coordination by hard acids (e.g., alkali metal cations) is principally an electrostatic interaction. As a consequence of Σ–CO– bonding, the CO stretching force constant of the interacting ligand decreases and that of the ancillary ligands increases. The strength of the interaction depends on the counter-cation electrostatic potential, as illustrated in Figure 12. Cotton–Kraihanzel force constants were calculated from the ν_{CO} spectra of the Li, Na, K,[30] and Al[26] salts of $[CpW(CO)_3]^-$ in THF; the Mg salt of $[CpMo(CO)_3]^-$ in THF;[29] and $NBu_4[CpW(CO)_3\cdot AlPh_3]$ in dichloromethane.[28] For each cation, the electrostatic potential (n^+/r_+) was calculated by dividing its formal positive charge by its effective crystal ionic radius in an octahedral

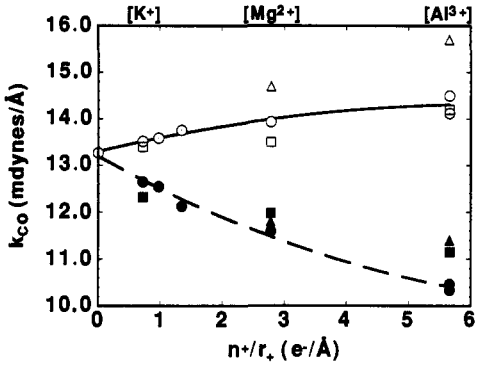

Figure 12. Correlations of the CO stretching force constants k_{iso} (filled symbols) and k_t (open symbols) with the counter-cation electrostatic potential: $[CpW(CO)_2(\Sigma\text{–}CO\text{–})]^-$ species in solution (circles), $[CpW(CO)_2(\Sigma\text{–}CO\text{–})]^-$ species on metal oxides (squares), and $[CpW(CO)(\Sigma\text{–}CO\text{–})_2]^-$ species on metal oxides (triangles).

coordination environment.[53] The y-intercept of each curve is defined by the CO force constant of the carbonyl ligands in C_{3v} $[CpW(CO)_3]^-$. This datum represents the weak, nonspecific interaction of $[CpW(CO)_3]^-$ with a bulky counter cation (e.g., PPN^+) with an effective electrostatic potential of 0. The Σ–CO– force constant, k_{iso}, decreases smoothly with n^+/r_+ from this limit to 10.34 mdyn/Å in $Al[CpW(CO)_3]_3$. The CO force constant of the two terminal ligands, k_t, increases with n^+/r_+, but the change in k_t is smaller than in k_{iso}.

The strength of the interaction of $[CpW(CO)_3]^-$ with Lewis acid centers on metal oxides is influenced similarly by the cation electrostatic potential (Figure 12). For the surface species which contain one Σ–CO– ligand, k_{iso} and k_t follow closely the same trends that are observed for solution ion pairs, but there are deviations which are diagnostic of the nature of metal carbonyl anion–Lewis acid adducts on metal oxide surfaces. The k_t values are systematically lower for the surface species, consistent with lower k_{ave} values and greater charge transfer to the carbonyl ligands. The k_{iso} values that characterize surface-bound $[CpW(CO)_3]^-$ on MgO and γ-Al_2O_3 are higher than expected for Mg^{2+} and Al^{3+} ion pairs, respectively, in solution, indicating weaker electrostatic interactions with carbonyl O atoms. Also, the Σ–CO-$\{Al^{3+}\}$ interaction is apparently weaker than the Σ–CO–$AlPh_3$ interaction in $NBu_4[CpW(CO)_3{\cdot}AlPh_3]$.[54] These results suggest that Mg and Al ions terminating the binary metal oxides have lower electrostatic potentials than Mg^{2+} and Al^{3+} ions, respectively, in nonpolar solutions. For Al ions, the difference is substantial, consistent with the greater electronegativity of Al and the more covalent character of its oxides. In contrast, K ions terminating γ-Al_2O_3 interact more strongly with $[CpW(CO)_3]^-$ than K^+ ions in solution, suggesting that the $\{K^+\}$ ions are highly exposed, perhaps as Al–OK groups.[51]

The k_{iso} values calculated for $\{M^{n+}\}_2[CpW(CO)(\Sigma\text{–}CO\text{–})_2]^-$ (M = Al, Mg) are nearly equal to those characterizing the respective $\{M^{n+}\}[CpW(CO)_2(\Sigma\text{–}CO\text{–})]^-$ (M = Mg, Al) ion adducts (Figure 12). This similarity suggests that in the bis-(isocarbonyl) species the two Σ–CO-$\{M^{n+}\}$ interactions are independent. The bis(isocarbonyl) interaction has a more pronounced effect on k_t, indicating that the charge-transfer effect is additive, as there are two Σ–CO– ligands and only one terminal CO ligand. The marked charge transfer away from the terminal carbonyl ligand is expected to weaken its W–C bond and facilitate ligand dissociation.[55]

(53) (a) Shannon, R. D.; Prewitt, C. T. *Acta Crystallogr.* **1969**, *B25*, 925. (b) Shannon, R. D.; Prewitt, C. T. *Acta Crystallogr.* **1970**, *B26*, 1046.

(54) Earlier work had indicated that the Lewis acid strength of $\{Al^{3+}\}$ on γ-Al_2O_3 toward the O atoms of bridging carbonyl ligands in neutral complexes ranked between that of $AlBr_3$ and $Al(C_2H_5)_3$ in solution: Tessier-Young, C.; Correa, F.; Ploch, D.; Burwell, R. L., Jr.; Shriver, D. F. *Organometallics* **1983**, *2*, 898.

(55) Otten, M. M.; Lamb, H. H. *J. Mol. Catal.* **1992**, *74*, 305.

Conclusions

Deprotonation of $[HCpW(CO)_3]$ on MgO, γ-Al_2O_3, and K/Al_2O_3 results in surface-bound $[CpW(CO)_3]^-$ complexes which interact with $\{M^{n+}\}$ counter cations via Σ–CO– ligands. Characterization of the surface-bound anions by EXAFS spectroscopy demonstrated that the structures are closely similar to those of crystallographically characterized cyclopentadienyltricarbonyltungstate(–1) model compounds. Isocarbonyl adducts containing one Σ–CO– ligand per complex are formed on each surface; these species are surface analogues of the contact ion pairs formed by $[CpW(CO)_3]^-$ with K^+, Mg^{2+}, and Al^{3+} ions in nonpolar solvents. A similar relationship is observed between the Σ–CO– stretching force constant and the electrostatic potential of the counter cation in solution and on metal oxide surfaces. Ion adducts containing two Σ–CO– ligands per complex are formed on MgO and γ-Al_2O_3. These species can be accommodated on ideal MgO(100) and Al_2O_3(111) surfaces by postulating that the $[CpW(CO)_3]$ moiety bridges neighboring $\{M^{n+}\}$ sites via Σ–CO– ligands. The bis-(isocarbonyl) adduct is obtained in high yield on γ-Al_2O_3 by *in vacuo* annealing of surface species derived by adsorption of $[HCpW(CO)_3]$ vapor. Dissociation of $\{Al^{3+}\}_2[CpW(CO)(\Sigma\text{–}CO\text{–})_2]^-$ to yield C_{3v} $[CpW(CO)_3]^-$ on γ-Al_2O_3 was demonstrated by exposure to pyridine vapor. Surface-bound $[CpW(CO)_3]^-$ was used to probe the surface composition of K/Al_2O_3; addition of 7.2 K^+/nm^2 to γ-Al_2O_3 effectively eliminated the interaction of $[CpW(CO)_3]^-$ with $\{Al^{3+}\}$ in favor of $\{K^+\}$.

Experimental Methods

Preparation of $[HCpW(CO)_3]$ and $[DCpW(CO)_3]$. $[HCpW(CO)_3]$ was prepared by the method of Piper and Wilkinson.[56] $[W(CO)_6]$ (8.8 g) (Strem) was heated with a 20% excess of $Na(C_5H_5)$ in refluxing tetrahydrofuran (THF) for 16 h. The solvent was removed *in vacuo* and the solid residue treated with excess glacial acetic acid in THF. The mixture was stirred for a few minutes at room temperature, and then the solvent was removed by evaporation. The crude product was separated from the reaction mixture by *in vacuo* sublimation onto an ice-cooled probe. To remove traces of $[W(CO)_6]$ (ν_{CO} = 1981 cm^{-1}), the hydride was purified by fractional sublimation, yielding bright yellow crystals. The infrared spectrum of the refined product (ν_{CO} = 2020 s, 1925 vs cm^{-1} (toluene solution)) is in agreement with that reported by Davidson, McCleverty, and Wilkinson.[57] $[DCpW(CO)_3]$ was prepared by substituting acetic acid-*d* for acetic acid in the above procedure.

Pretreatment of Metal Oxides. MgO (MX-65-1, MCB Reagents) was outgassed *in vacuo* for 8–10 h at 800 °C; the BET surface area of the resultant powder was 39 m^2/g. Nonporous γ-Al_2O_3 (Degussa Aluminum Oxide C) was wetted with deionized water to form a paste that was subsequently dried in air. Samples then were crushed and pretreated at 400 and 800 °C *in vacuo* for 8–10 h; the BET surface areas of the resultant powders were 100 and 76 m^2/g, respectively. K/Al_2O_3 samples were produced by treating Degussa γ-Al_2O_3 (7.0 g) with KNO_3 solutions in deionized water (150 mL). The resultant suspensions were evaporated to dryness over low heat, ground, and heated at 800 °C *in vacuo* for 8–10 h. The potassium loadings were equivalent to 1.5 and 6.5 K^+/nm^2 of starting γ-Al_2O_3 surface; the BET surface areas of the resultant K/Al_2O_3 powders were 95 and 90 m^2/g, respectively.

Chemisorption of $[HCpW(CO)_3]$. Samples of the metal oxides (3.0 g) were contacted with solutions of $[HCpW(CO)_3]$ or $[DCpW(CO)_3]$ (82 mg) in toluene (75 mL, freshly distilled from Na/benzophenone) for 2 h at 25 °C under N_2 and in the dark. Samples with one-half the typical W loading on MgO were prepared using $[DCpW(CO)_3]$ (41 mg). The resultant light yellow solids were recovered by filtration, washed with fresh toluene (50 mL), and dried. Aliquots of the toluene solutions were examined by infrared spectroscopy before and after contact with the metal oxides, and adsorbed amounts were estimated from the observed decrease in $[HCpW(CO)_3]$ ν_{CO} bands. The samples were stored in glass vials wrapped in Al foil in an mBraun drybox.

$[HCpW(CO)_3]$ vapor was adsorbed on γ-Al_2O_3 pretreated *in vacuo* at 800 °C. Self-supporting wafers were pressed in a drybox and loaded

(56) Piper, T. S.; Wilkinson, G. *J. Inorg. Nucl. Chem.* **1956**, *3*, 104.

(57) Davison, A.; McCleverty, J. A.; Wilkinson, G. *J. Chem. Soc.* **1963**, 1133.

into an *in situ* infrared spectroscopy cell. After evacuation of N_2 using a turbomolecular pump, a wafer was exposed to $[HCpW(CO)_3]$ vapor emanating from a source tube containing pre-purified crystals at 25 °C. The wafer temperature was 25 °C. An exposure cycle of 5 min was followed by evacuation for 5 min; five cycles for a cumulative exposure time of 25 min were made. After the final exposure cycle, the wafer was heated *in vacuo* at 50, 70, and 100 °C.

Solubilization of Surface-Bound Anions. Self-supporting wafers of $[HCpW(CO)_3]$ adsorbed on the metal oxides were contacted with solutions of $[PPN][Cl]$ ($[PPN]^+ = [N(PPh_3)_2]^+$) in CH_2Cl_2 (2–3 mL) at 25 °C under N_2. After approximately 1 h, the supernatant solutions and the wafers (after rinsing with fresh dichloromethane) were examined by infrared spectroscopy. CH_2Cl_2 was dried over 4-Å molecular sieves (activated at 400 °C *in vacuo*).

Infrared Spectroscopy. Infrared spectra were obtained with an Analect FX-6260 Fourier transform spectrometer; the spectral resolution was 4 cm^{-1}. Metal oxide powders (70–90 mg) were pressed in the drybox in a 19-mm circular die at 13 kN to yield thin self-supporting wafers, which were loaded into gas-tight cells fitted with NaCl or CaF_2 windows. Cells could be connected to a gas-handling manifold for evacuation and for dosing of gases and vapors; the base pressure of the turbomolecularly pumped manifold was 10^{-6} Torr.

Pyridine Dosing. Wafers of $[HCpW(CO)_3]$ adsorbed on γ-Al_2O_3 were exposed to pyridine vapor at 25 °C; the pyridine pressure was measured using a capacitance manometer. Infrared spectra were recorded after a 10-min exposure at a given pressure. Pyridine was degassed by three freeze–pump–thaw cycles.

X-ray Absorption Spectroscopy (XAS). XAS measurements were made on the Beamline X-11A at the National Synchrotron Light Source (NSLS) at Brookhaven National Laboratory. The storage-ring energy was 2.5 GeV, and the current decayed from 200 to 100 mA during a typical fill. The monochromator was equipped with a pair of Si(111) crystals. Spectra were recorded in the region of the W L_{III} absorption edge (10.207 keV) in transmission mode.

Samples (150–200 mg) of $[HCpW(CO)_3]$ adsorbed on MgO, γ-Al_2O_3, and K/Al_2O_3 were pressed into stainless steel holders and installed under N_2 in XAS cells equipped with Be windows.[58] The cells were then evacuated and pressurized with ultra-high-purity He. Spectra were measured with the samples cooled to approximately −173 °C. Spectra of $[W(CO)_6]$ crystals mixed in BN and $[CpW(CO)_3]_2$ crystals mixed in BN were also measured at approximately −173 °C. At least two energy scans of each sample were obtained; the replicate data sets were averaged.

The W L_{III} extended X-ray absorption fine structure (EXAFS) spectra were isolated from the raw XAS data by pre-edge subtraction followed by cubic spline fitting and subtraction.[59] The EXAFS spectra were analyzed using phase-shift and backscattering functions derived from reference compounds. The experimental EXAFS spectrum of $[W(CO)_6]$ was used to obtain W–C and W–O* references, which were used in fitting W–C, W–C*, and W–O* contributions. The W–C and W–O* references were generated by Fourier-filtering of the $[W(CO)_6]$ EXAFS (forward transform, k^2 weighting, $2.6 \le k \le 15.2$ Å^{-1}; back transforms, W–C, $0.86 \le r \le 2.16$ Å and W–O*, $2.16 \le r \le 3.40$ Å). A reference derived from the EXAFS spectrum of Re powder was used in fitting the W–W contribution of the EXAFS spectrum of $[CpW(CO)_3]_2$.

For $[HCpW(CO)_3]$ adsorbed on MgO, γ-Al_2O_3, and K/Al_2O_3, the first-shell EXAFS contributions were isolated by Fourier-filtering (k^2 weighting, $2.9 \le k \le 13$ Å^{-1}, $0 \le r \le 3.4$ Å) and were fitted using k^2 weighting ($3.5 \le k \le 12.5$ Å^{-1}). For crystalline $[CpW(CO)_3]_2$ the data were Fourier-filtered (k^2 weighting, $3.4 \le k \le 15$ Å^{-1}, $0 \le r \le 3.5$ Å) and were fitted using k^2 weighting ($4 \le k \le 14$ Å^{-1}).

Acknowledgment. This research was supported by an NSF Presidential Young Investigator Award (CTS-8958350) and matching contributions from Hoechst Celanese Corporation. The authors wish to acknowledge Professor B. C. Gates and M. Nagle of the University of Delaware and K. Clawson and B. Colvin of North Carolina State University for their contributions to this work. X-ray absorption spectroscopy research was carried out at the National Synchrotron Light Source, Brookhaven National Laboratory, which is supported by the U. S. Department of Energy, Division of Materials Sciences and Division of Chemical Sciences (DOE contract DE-AC02-76CH00016). We thank the operating staff of Beamline X-11 for their assistance.

(58) Kampers, F. W. H.; Maas, T. M. J.; vanGrondelle, J.; Brinkgreve, P.; Koningsberger, D. C. *Rev. Sci. Instrum.* **1989**, *60*, 2635.

(59) Sayers, D. E.; Bunker, B. A. In *X-Ray Absorption: Principles, Applications. Techniques of EXAFS. SEXAFS and XANES*; Koningsberger, D. C., Prins, R., Eds.; Wiley: New York, 1988.